Narasimhan, V., & Bryan, A. M. (1984) *Experientia 40*, 827–828.
Nordheim, A., Lafer, E. M., Peck, L. J., Wang, J. C., Stollar, B. D., & Rich, A. (1982) *Cell 31*, 309–318.
Peck, L. J., & Wang, J. C. (1983) *Proc. Natl. Acad. Sci. U.S.A. 80*, 6206–6210.
Pohl, F. M. (1976) *Nature 260*, 365–366.
Pohl, F. M., & Jovin, T. M. (1972) *J. Mol. Biol. 57*, 375–395.
Rich, A., Nordheim, A., & Wang, A. H.-J. (1984) *Annu. Rev. Biochem. 53*, 791–846.
Saenger, W., Hunter, W. N., & Kennard, O. (1986) *Nature 324*, 385–388.
Soumpasis, D. M. (1984) *Proc. Natl. Acad. Sci. U.S.A. 81*, 5116–5120.
Tidor, B., Irikura, K. K., Brooks, B. R., & Karplus, M. (1983) *J. Biomol. Struct. Dyn. 1*, 231–252.
Vologodskii, A. V., & Frank-Kamenetskii, M. D. (1984) *J. Biomol. Struct. Dyn. 1*, 1325–1333.
Vorlickova, M., & Jaroslav, K. (1984) *Int. J. Biol. Macromol. 6*, 77–80.
Wang, A. H.-J., Quigley, G. J., Kolpak, F. J., Crawford, J. L., van Boom, J. H., van der Marel, G. A., & Rich, A. (1979) *Nature 282*, 680–686.
Wang, A. H.-J., Quigley, G. J., Kolpak, F. J., van der Marel, G. A., van Boom, J. H., & Rich, A. (1981) *Science 211*, 171–176.
Wang, A. H.-J., Hakoshima, T., van der Marel, G., van Boom, J. H., & Rich, A. (1984) *Cell 37*, 321–331.
Warner, H. R., Duncan, B. K., Garrett, C., & Neuhard, J. (1981) *J. Bacteriol. 145*, 687–695.

Binding of Mithramycin to DNA in the Presence of Second Drugs†

Matilal Sarker and Fu-Ming Chen*
Department of Chemistry, Tennessee State University, Nashville, Tennessee 37209-1561
Received February 14, 1989; Revised Manuscript Received May 2, 1989

ABSTRACT: Comparative DNA equilibrium binding studies with mithramycin (MTR) and ethidium bromide in the presence and in the absence of second drugs were investigated by spectral titrations. Unusual curvatures (in contrast to those due to neighbor exclusion or anticooperativity) are found in the Scatchard plots of MTR–DNA titrations in the presence of netropsin, a minor-groove binder. Parallel studies with ethidium bromide indicate that although the presence of netropsin significantly reduces the binding ability of ethidium, no unusually curved Scatchard plots are obtained. The unusual curvature exhibited by the Scatchard plots of MTR titrations in the presence of netropsin indicates that the binding of netropsin greatly affects the MTR binding to DNA and can be simulated by an explicit incorporation of the second drug–DNA interaction in the binding formalism. Since netropsin is a minor-groove binder, its interference with the binding of MTR is in accord with the notion that MTR also binds at this groove. The observation of negligible effects on the DNA binding ability of MTR in the presence of either a major-groove or a phosphate group binder lends further support to this conclusion. Consistent with its guanine specificity, studies with synthetic polynucleotides suggest that MTR exhibits negligible affinity for poly(dA-dT)·poly(dA-dT) or poly(dA)·poly(dT). Although the strongest bindings are demonstrated by poly(dG-m^{5}dC)·poly(dG-m^{5}dC), poly(dG-dC)·poly(dG-dC), and poly(dG)·poly(dC), the homopolymer exhibits a saturation density of approximately 1 drug molecule per every 2–3 base pairs, whereas the alternating polymers saturate at 1 drug molecule per <2 base pairs, a rather surprising finding for such an extended molecule but one consistent with the drug–dimer model on binding. The effect of sequence or conformation on the binding is further indicated by the stronger MTR affinity for poly(dA-dG)·poly(dC-dT) than for poly(dA-dC)·poly(dG-dT). These results are supported by circular dichroic measurements.

Mithramycin (MTR) is an antibiotic that contains an aureolic acid group and is closely related to chromomycin A_3 and olivomycin. Some studies on this drug, mainly clinical, have been made in recent years (Gause, 1965; Kennedy et al., 1968; Ream et al., 1968; Kennedy, 1970; Hill et al., 1972; Prasad & Nayak, 1976; Dasgupta et al., 1979; Fox & Howarth, 1985). Despite its high toxicity, this drug has proved useful for treating patients with testicular carcinomas (Ream et al., 1968; Kennedy, 1970; Hill et al., 1972) and Paget's disease (Elias et al., 1972). MTR inhibits the synthesis of both DNA and RNA in vivo, with some preference for the latter (Kersten et al., 1967; Fok & Waring, 1972). For its DNA binding, this antibiotic exhibits an absolute requirement for divalent cations such as Mg^{2+} (Behr & Hartmann, 1965; Goldberg & Friedman, 1971). This drug is anionic above neutral pH (Illrionova et al., 1970) and exhibits guanine specificity in DNA (Ward et al., 1965; Behr et al., 1969). Its fluorescence intensity at certain wavelengths is greatly enhanced upon binding to DNA, thus enabling this compound to be used in microfluorometric analysis of cellular DNA (Coleman & Goff, 1985; Hauser-Urfer et al., 1982; Coleman et al., 1981; Hamilton et al., 1980; Groyer & Robel, 1980; Buys & Osinga, 1980). Footprinting experiments have shown that the preferred binding sites of MTR and its related antibiotics are at least 3 base pairs long (Fox & Howarth, 1985; Van Dyke & Dervan, 1983). The mode of interaction of this class of drugs, however, has not yet been unequivocally established.

It is generally believed that MTR binds nonintercalatively at the minor groove of DNA. This stems from the observations by several investigators that MTR fails to affect some prop-

† Research supported by USPHS Grant CA-42682 and by a subproject of MBRS Grant S06RR0892.

0006-2960/89/0428-6651$01.50/0

erties of DNA such as sedimentation coefficient, viscosity, or melting temperature (Goldberg & Friedman, 1971; Kersten et al., 1966) and exhibits little effect on the supercoiling of DNA (Waring, 1970). Circular dichroism studies by Dalgleish et al. (1974) on the complexes of DNA with MTR and related drugs have shown that MTR and chromomycin A_3 have very similar binding sites, although it was not possible to predict whether these drugs intercalate in DNA or not. Some workers, however, have indicated that MTR does in fact partially intercalate between DNA base pairs in a magnesium-dependent fashion (Prasad & Nayak, 1976; Dasgupta et al., 1979; Nayak et al., 1973). In contrast, an NMR study with d(ATGCAT) led Keniry et al. (1987) to suggest that chromomycin A_3 may bind at the major groove of DNA. The possibility of a major-groove binding of MTR had also been raised earlier by Fox and Howarth (1985).

Our interest in these aureolic acid antibiotics stems in part from their slow DNA dissociation kinetics (Behr et al., 1969), similar to those exhibited by actinomycin D, which has been credited for their pharmacological effect (Muller & Crothers, 1968). Since MTR and its closely related antibiotics are G·C rather than A·T specific, as exhibited by almost all other nonintercalative minor-groove binders, their DNA binding characteristics will, thus, be of particular interest. Although some DNA equilibrium binding studies of chromomycin A_3 had been reported (Behr et al., 1969; Nayak et al., 1973, 1975), few systematic investigations on MTR had been made. To gain insights into its binding mode, MTR binding to DNA has been investigated in the absence and in the presence of minor-groove-binder netropsin, phosphate backbone binders methylviologen and benzylviologen, and major-groove–phosphate binders spermidine and spermine (Drew & Dickerson, 1981; Absu et al., 1987; Marquet & Houssier, 1988). These results are then compared with some ethidium bromide measurements.

Spectroscopic titrations of MTR have also been carried out with synthetic polynucleotides in an effort to elucidate the effect due to sequence and/or conformation on the binding. The data were analyzed by the McGhee and von Hippel (1974) model with or without cooperativity. The puzzling high-saturation binding densities found for some polynucleotides were then rationalized in terms of the notion of a drug dimer binding to DNA, as suggested by a most recent NMR study on a chromomycin A_3–oligomer system (Gao & Patel, 1989).

Materials and Methods

Mithramycin A (MTR), methylviologen dichloride (MV), and benzylviologen dichloride (BV) were purchased from Aldrich and used without further purification. The stock solutions of these drugs were prepared in a 10 mM Tris-HCl buffer of pH 8 containing 10 mM NaCl. The concentrations of stock MV and BV solutions were determined by weight, while that of MTR was determined spectroscopically by using an extinction coefficient of 10000 cm^{-1} M^{-1} at 400 nm. All experiments were carried out in the same buffer. Ethidium bromide (EB) was purchased from Sigma, and the concentration of its stock solution in the pH 8 buffer was determined with an extinction coefficient of 5850 cm^{-1} M^{-1} at 480 nm. Netropsin (NT) was purchased from Serva, and its stock concentration was determined by weight. Calf thymus DNA (CT DNA) was purchased from Sigma and deproteinized by extractions with 24:1 (v/v) chloroform:isoamyl alcohol mixtures (Muller & Crothers, 1975). The concentration of the stock DNA solution (in nucleotide) was determined with an extinction coefficient of 6550 cm^{-1} M^{-1} at 260 nm. Spermidine (SPD) and spermine (SPM) were purchased from Serva and their concentrations determined by weight.

Absorption spectra were measured at 22–24 °C with a Cary 210 spectrophotometric system equipped with a Neslab RTE-8 refrigerated circulating bath. The stirrer accessory was used during the absorption spectral titrations. Fluorescence measurements were carried out with a Jasco FP 550 spectrofluorometer. Emission spectral changes were monitored at 540 nm for excitation at the isosbestic wavelength of 410 nm, using 3 and 5 nm as excitation and emission slit widths, respectively. Circular dichroism (CD) spectra were measured by a Jasco J-500A recording spectropolarimeter at room temperature.

Results

Equilibrium Binding of Mithramycin to DNA in the Absence of Other Drugs. The requirement for divalent cations such as Mg^{2+} for the DNA binding of MTR is well-known. MTR exhibits an absorption maximum at 400 nm and a shoulder around 425 nm. Addition of DNA in the absence of magnesium scarcely alters the spectrum in the drug region. Successive additions of $MgCl_2$ result in progressive spectral alterations that eventually result in a much broader spectrum with the maximum red shifted by 20 nm (not shown). An isosbestic point is maintained at 410 nm. To determine the optimal concentration of Mg^{2+} needed in spectral titrations, a solution containing 10 μM MTR and 0.16 mM CT DNA was titrated by a progressive addition of concentrated $MgCl_2$ solution. The results indicate that the presence of a 0.25 mM Mg^{2+} accomplishes a 95% spectral alteration. No further changes were evident when the magnesium concentration was above 0.4 mM. Consequently, all our spectral titrations were carried out in the presence of 0.5 mM magnesium chloride.

The absorption spectral titrations were carried out by progressive additions of a concentrated DNA stock into a drug solution (10 μM, unless stated otherwise). Due to its slow rate of association, a 30-min waiting period was allowed after each addition. Absorption spectral changes in the drug spectral region are similar to those for the Mg^{2+} titrations described above, with a reasonably clean isosbestic point maintained at 410 nm. Absorbance changes at 440 and 400 nm were used to arrive at the binding isotherms. These absorbance values, in conjunction with the total drug concentrations, were used to calculate the fraction of drug bound as $(e - e_f)/(e_b - e_f)$, where e, e_b, e_f are the apparent, bound, and free drug extinction coefficients, respectively. The data were initially analyzed according to the Scatchard equation $r/m = K_a(s - r)$ and two other equivalent forms (Klotz & Hunston, 1971), $1/r = 1/s + (1/sK_am)$ and $m/r = 1/sK_a + (m/s)$, where r is the ratio of bound drug and DNA base pair concentrations, s is the number of binding sites per base pair, K_a is the apparent association constant, and m is the free drug concentration. Our experience suggests that the use of absorbance differences between 440 and 400 nm results in a less scattered plot than the use of absorbance values of a single wavelength, and consequently, such a practice was implemented throughout.

Since most of our Scatchard plots appear to be linear in the high DNA concentration region, the following scheme was adopted for extracting the best bound extinction coefficients: (1) an initial bound extinction coefficient was obtained through an extrapolation in a $1/(e - e_f)$ vs $1/([DNA]_{bp} - C_t)$ plot (Benesi & Hildebrand, 1949; Schmechel & Crothers, 1971), where C_t denotes the total drug concentration; (2) this value was then used to obtain a $1/r$ vs $1/m$ plot; (3) the data points with high DNA concentrations were then subjected to a linear regression analysis; (4) new e_b values were then tried and the coefficients of correlation compared; (5) the e_b that gave the

Table I: Summary of Binding Parameters Extracted from McGhee–von Hippel Analysis

DNA	drug[a]	second drug (μM)	K^b (1/μM)	n^b (bp/drug)	K	n	w
CT DNA	MTR		0.27	3.3	0.27	2.8	0.4
CT DNA	MTR	NT (10)	0.2[c]	5.9[c]			
CT DNA	MTR	MV (100)	0.18	2.9			
CT DNA	MTR	BV (100)	0.17	3.0			
CT DNA	MTR	SPD (10)	0.20	2.4			
CT DNA	MTR	SPM (10)	0.29	2.5			
CT DNA	EtBr		2.0	2.1	2.4	1.9	0.6
CT DNA	EtBr	NT (10)	0.29	2.2	0.33	1.7	0.3
CT DNA	EtBr	NT (100)	0.05	2.1	0.05	1.6	0.4
CT DNA	EtBr	MV (100)	0.68	2.1			
CT DNA	EtBr	BV (100)	0.58	1.9			
poly(dG)·poly(dC)	MTR (5)		1.1	2.7	0.83	2.9	1.8
poly(dG)·poly(dC)	MTR (5)	NT (10)	0.77	2.6			
poly(dG-dC)·poly(dG-dC)	MTR		1.3	1.6	1.1	1.8	1.6
poly(dG-dC)·poly(dG-dC)	MTR	NT (10)	0.74	1.6			
poly(dA-dG)·poly(dC-dT)	MTR		0.30	2.5	0.23	2.9	2.1
poly(dA-dC)·poly(dG-dT)	MTR		0.03	5.4	0.03	4.9	0.5
poly(dG-m^{5}dC)	MTR (5)		1.81	1.7	1.7	1.8	1.2

[a] Titrations were made by starting with a MTR or EB concentration of 10 μM, except for the ones followed by (5), indicating 5 μM concentration. [b] Parameters extracted by using the noncooperative neighbor exclusion model of McGhee and von Hippel (1974). For the sake of comparison, some titrations have also been subjected to analysis by a cooperative model with the results shown in the last three columns. [c] Values estimated from the linear portion of the Scatchard plot.

best correlation coefficient was then used for plotting the binding isotherms, and the binding parameters for strong sites were extracted through linear regression analysis. The choice of $1/r$ vs $1/m$ for such a purpose is made on the basis of the fact that this plot spreads out the data points of higher DNA concentrations to a greater extent and the fact that the parameters for strong binding sites rely more heavily on these points.

A typical Scatchard plot for the MTR titration in the absence of a second drug is shown as part of Figure 1. The curvature observed in the region of larger r may be attributed to either binding at weaker sites or neighbor exclusion and/or anticooperative effects. The binding equation derived by McGhee and von Hippel (1974), including both the neighbor exclusion and cooperative effects, is

$$r/m = K(1 - nr)\{[(2w - 1)(1 - nr) + r - R]/[2(w-1) \times (1 - nr)]\}^{n-1}\{[1 - (n + 1)r + R]/[2(1 - nr)]\}^2$$

with R defined as $\{[1 - (n + 1)r]^2 + 4wr(1 - nr)\}^{1/2}$ and w being the cooperative factor. In the absence of cooperativity (in the limit of $w \rightarrow 1$), the equation simplifies to

$$r/m = K(1 - nr)\{(1 - nr)/[1 - (n - 1)r]\}^{n-1}$$

where K is the site binding constant and n is the binding site size. It should be pointed out that the usual Scatchard values and the McGhee and von Hippel parameters are related by $K_a = Kn$ and $n = 1/s$.

Our titration data were subjected to nonlinear least-squares fits with both equations, using the results of simple Scatchard analyses as starting values, and the extracted binding parameters for the MTR–DNA studies are summarized in Table I along with other results that are discussed in later sections. As can be seen, a binding constant of approximately 0.3×10^6 M^{-1} and a saturation binding density of 1 drug molecule per 3.3 bp have been extracted for the MTR–CT DNA titration. These values compare favorably with literature values for the related drug chromomycin A_3 obtained under different experimental conditions (Behr et al., 1969; Nayak et al., 1973).

Scatchard Plots of Mithramycin–DNA Binding in the Presence of Netropsin. To investigate the effect of netropsin on the MTR binding to DNA, spectral titrations were also made in the presence of 10 and 100 μM netropsin. The resulting Scatchard plots along with that of MTR alone are presented in Figure 1. As is apparent, the Scatchard features

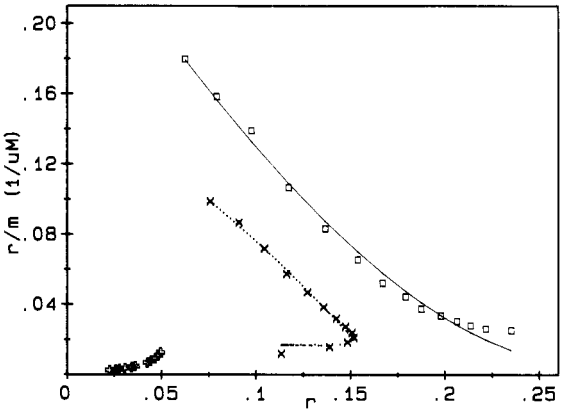

FIGURE 1: Comparison of mithramycin–DNA Scatchard plots in the absence (squares) and in the presence of 10 μM (×) and 100 μM (+) netropsin. Titrations were made at 23 °C with a starting MTR concentration of 10 μM in a pH 8 buffer containing 10 mM NaCl, and absorbance differences between 440 and 400 nm have been used to construct the binding isotherms. The theoretical curve (dots) for the titration in the presence of 10 μM NT was calculated from eq 1 with $K_a = 0.45$, $K_b = 0.66$ μM^{-1}, and $s = 0.38$. The solid curve is the nonlinear least-squares fit for the titration in the absence of second drugs, using the McGhee and von Hippel equation with cooperativity (see Table I for the fitting parameters).

in the presence of netropsin are distinctly different from that of MTR alone. For the titration in the presence of 10 μM netropsin, r initially increases but eventually decreases (normal Scatchard plot) as r/m is increased. For titrations in the presence of 100 μM netropsin, the portion exhibiting the normal Scatchard plot (r/m increases as r is decreased) was never reached.

To explain these unusual features, the following theoretical model using the formalism of simple Scatchard analysis has been considered. In the presence of two drugs A (MTR) and B (netropsin), the two equilibria are in order

$$P + A = PA \quad \text{with } K_a = [PA]/[P][A]$$

$$P + B = PB \quad \text{with } K_b = [PB]/[P][B]$$

which yield the relation $K_a/K_b = [PA][B]/[PB][A]$. Replacing [B] with B_t − [PB] and rearranging, one obtains

$$[PB] = B_t/(K_a[A]/K_b[PA] + 1)$$

If N is the total DNA concentration in base pair and s is the number of binding sites per base pair for each of the two

ligands, obviously a simplifying assumption, the first equilibrium can then be rewritten as

$$K_a = [PA]/(sN - [PA] - [PB])[A]$$

since [P] is the concentration of binding sites that are still free, i.e., total binding sites minus the sites occupied by A and B. Rearranging and dividing both sides by N yield

$$K_a(s - r - [PB]/N) = r/m$$

where $r = [PA]/N$ by definition and $m = [A]$, the free drug concentration of A. Finally, replacing [PB] in the expression results in

$$K_a(s - r - B_t/(N + mK_a/rK_b)) = r/m \qquad (1)$$

It is reassuring that in the absence of drug B the expression reduces to the Scatchard equation for drug A alone. It is also apparent from the equation that in the presence of a second drug one has to increase the DNA concentration to compensate for the contribution from the extra term in the equation.

It is noted from eq 1 that if a plot of $r + B_t/(N + mK_a/rK_b)$ vs r/m is made with an appropriate choice of K_a/K_b, one may secure a straight line with a slope K_a and an ordinate intercept sK_a. A computer program was written for such a plot with a keyboard input of the ratio of binding constants. Approximate binding parameters obtained were then used as starting values for a nonlinear least-squares fit. The binding parameters extracted from such a fit for titrations in the presence of 10 μM netropsin are given in the figure legend and the calculated binding isotherm is compared with the experimental data in Figure 1. It is gratifying to see that the unusual curvature can be simulated fairly well. Extraction of reasonable binding parameters from the titration in the presence of 100 μM netropsin, however, proved unfeasible, as data points in the "normal" Scatchard region were never attained.

Comparison with the Binding Isotherms of Ethidium Bromide. In the absence of DNA, EB exhibits an absorption maximum at 480 nm. A hypochromic effect and a concomitant red shift of 40 nm occur as it binds to DNA, while an isosbestic point at 506 nm is maintained. Scatchard plots for DNA binding to EB in the absence and in the presence of netropsin, using the differential absorbances of 520 and 480 nm, are shown in Figure 2. It is apparent that the presence of netropsin also greatly affects the binding of EB to DNA. In contrast to MTR, however, the effect of netropsin on the EB binding only results in significant changes in slopes of the Scatchard plots without the introduction of unusual curvatures as seen in the MTR titrations. Binding parameters obtained for EB titrations are also shown in Table I. As is apparent, the presence of 100 μM netropsin reduces the binding constant by nearly 40-fold, yet the n value remains at 2. Our binding constant of about 2 μM^{-1} for EB in the absence of netropsin and n of approximately 2 compare favorably with the literature values (LePecq & Paoletti, 1967).

Effects of Non-Minor-Groove Binders on the DNA Binding of MTR. MV^{2+} (1,1′-dimethyl-4,4′-bipyridinium ion) is known to bind to DNA, and its mode of binding is suspected to be predominantly at the phosphate backbone with an approximate binding constant of 0.2 μM^{-1} and $n = 1$ (Fromher & Reiger, 1986). This compound has been used extensively in electron-transfer studies. BV^{2+} is a related compound with benzyl groups replacing the methyls, and its DNA binding characteristics are expected to be not very different from those of MV^{2+}. Spectral titrations of MTR and EB in the presence of MV and BV were thus carried out to see if they behave differently from the minor-groove-binding netropsin. Indeed,

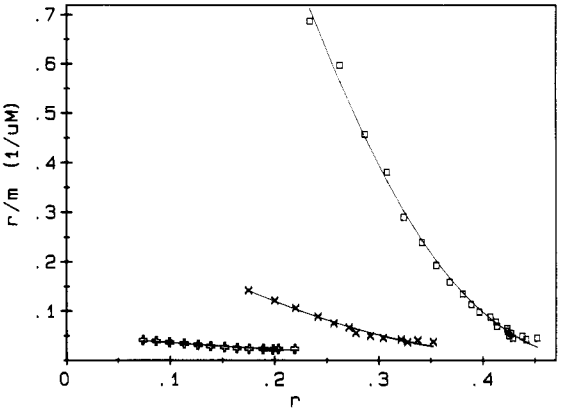

FIGURE 2: Comparison of ethidium–DNA Scatchard plots in the absence (squares) and in the presence of 10 μM (×) and 100 μM (+) netropsin. Differential absorbances between 520 and 480 nm have been used to construct the binding isotherms. Solid curves represent the nonlinear least-squares fits using the McGhee and von Hippel equation including cooperativity with the fitting parameters shown in Table I.

in contrast to netropsin, the presence of MV or BV as high as 100 μM does not appear to greatly affect either the apparent binding constants or the n values of the two drugs studied, as can be seen from Table I.

Spectral titrations with DNA have also been made for mithramycin in the presence of a major-groove binder spermidine or spermine. As can be seen in Table I, their presence at 10 μM does not appear to greatly alter the binding constant and only slightly affects the saturation density. Although titrations in the presence of 100 μM have also been attempted, the results are marred by aggregate formation. It should be pointed out that the exclusive major-groove binding of spermine and spermidine has not been conclusively established in solutions, and there are indications that their binding is characterized by high mobility along the DNA (Ware et al., 1988). Their binding affinity may further be complicated by their pK_a being near 8, the pH in which all measurements have been made.

Binding Studies with Fluorescence Titrations. In the buffer solution and in the presence of 0.5 mM Mg^{2+}, MTR exhibits a broad fluorescence emission spectrum with a maximum at 540 nm when the sample is excited with 400-nm light. The presence of DNA in the solution causes the fluorescence intensity around 540 nm to decrease. A concomitant increase in the 470-nm region results in a much broader emission spectrum. Excitation spectra of MTR in the absence and in the presence of DNA resemble closely those of absorption spectra in terms of red shifts and hypochromic effects. Fluorescence titrations of MTR with CT DNA were carried out in the absence and in the presence of netropsin by monitoring the fluorescence intensity at 540 nm while exciting at the isosbestic wavelength of 410 nm. Stern–Volmer plots of these titrations are shown in Figure 3. It is apparent that initially $I(0)/I$ increases linearly with increasing P/D but soon reaches a plateau and begins a slight decline at higher DNA concentrations. The intersection of the two straight-line portions can serve as a rough indication of the saturating P/D ratio. For the solution containing MTR alone, the intersection occurs at a P(bp)/D ratio of 3, while in the presence of 10 μM NT it increases to 5; in the presence of 100 μM NT the declining portion was never reached. The calculated values of the Stern–Volmer constants obtained from the slopes of ascending portions of the plots are 26, 15, and 3.6 mM^{-1} for MTR, MTR plus 10 μM NT, and MTR plus 100 μM NT,

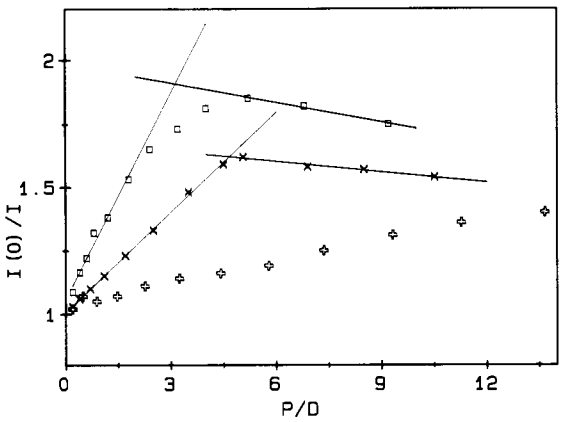

FIGURE 3: Comparison of Stern–Volmer plots for the MTR–DNA titrations in the absence (squares) and in the presence of 10 μM (×) and 100 μM (+) netropsin. Excitation and emission wavelengths are at 410 and 540 nm, respectively. Solid lines are linear least-squares fits for the linear ascending and descending portions of the data.

respectively, in agreement with the trend observed in absorbance titrations.

If the fluorescence data are employed for the Scatchard plot by using the molar fluorescence intensity at the intersection as the bound value, it is found that a maximum is exhibited at $r \sim 0.2$ for the 10 μM MTR solution and decreases to about 0.15 in the presence of 10 μM netropsin (results not shown). The estimated binding constants from the linear portions of the plots are also in general agreement with those obtained by absorbance titrations. It should be pointed out that the presence of a maximum in the Scatchard plot is likely the consequence of concentration-dependent quenching effects [which cause the decline in $I(0)/I$ at higher P/D] rather than that of cooperativity.

Binding Studies with Synthetic Polynucleotides. The sequence-specific binding of mithramycin was investigated by equilibrium binding studies with various synthetic polynucleotides. These results are also included in Table I. Consistent with the guanine specificity of MTR, binding to the two A·T polymers are quite weak and thus not shown. Binding strengths of the two G·C polymers, however, are nearly identical (1.1–1.3 μM^{-1}) except for the higher saturation binding density for the alternating polymer poly(dG-dC)·poly(dG-dC), 1 drug molecule bound per 1.6 base pairs as compared to 2.7 bp for the homopolymer poly(dG)·poly(dC). Binding to poly(dG-m^{5}dC)·poly(dG-m^{5}dC) appears to be slightly stronger than its unmethylated counterpart, but the high binding densities are quite comparable. Consistent with the A·T specificity of netropsin, the presence of 10 μM netropsin only slightly affects the MTR binding ability of either poly(dG-dC)·poly(dG-dC) or poly(dG)·poly(dC) without altering the saturation binding densities. Although the MTR binding ability of poly(dA-dG)·poly(dC-dT) is only 3–4-fold weaker than that of the two G·C polymers, it is an order of magnitude higher than its sequence isomer poly(dA-dC)·poly(dG-dT). The weaker binding ability of poly(dA-dC)·poly(dG-dT) is accompanied by a saturation density of 1 drug molecule per 5–6 base pairs, a factor of 2 lower than that of its sequence isomer poly(dA-dG)·poly(dC-dT). The binding isotherms of these polynucleotides along with the nonlinear least-squares fits using the McGhee and von Hippel equation without cooperativity are shown in Figure 4. It should be pointed out that the inclusion of the cooperative factor in the McGhee and von Hippel analysis does not usually improve the fit. Although too much significance should not be attached to the extracted cooperative factor, it is interesting to note that

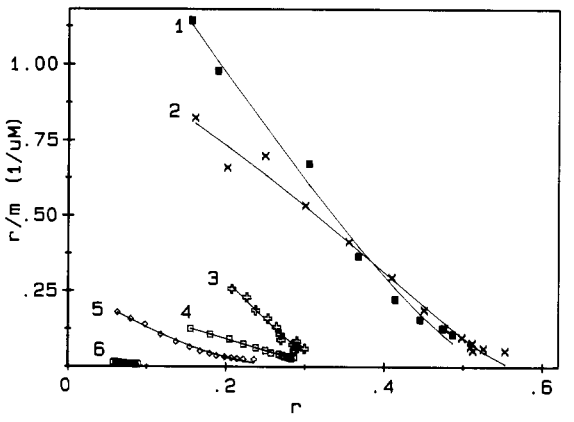

FIGURE 4: Scatchard plots resulting from titrations of mithramycin with various synthetic polynucleotides. Solid curves are the nonlinear least-squares fits using the McGhee and von Hippel equation without cooperativity. The fitted parameters can be found in Table I. (1) poly(dG-m^{5}dC)·poly(dG-m^{5}dC); (2) poly(dG-dC)·poly(dG-dC); (3) poly(dG)·poly(dC); (4) poly(dA-dG)·poly(dC-dT); (5) CT DNA; (6) poly(dA-dC)·poly(dG-dT).

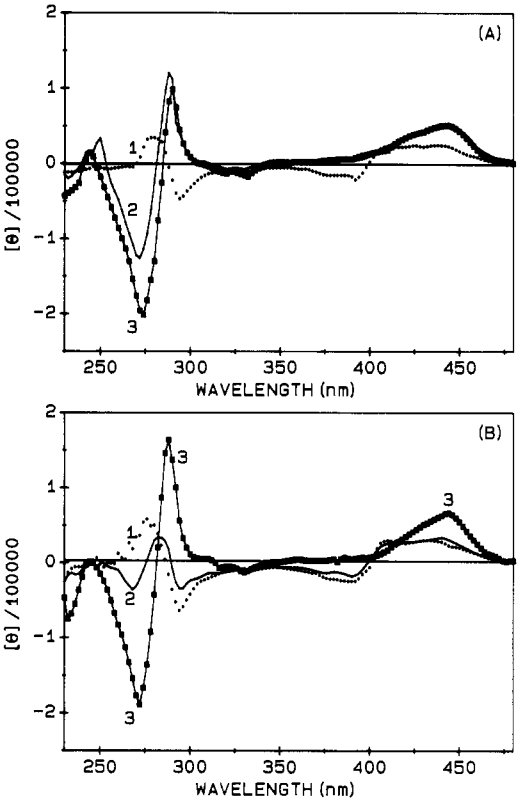

FIGURE 5: Comparison of difference CD spectra of 5 μM mithramycin in various polynucleotide solutions of 20 μM. Contributions due to polynucleotides in the absence of drug have been subtracted. Measurements were made with a 2-cm cylindrical cell at room temperature. (A) pH 8 buffer (dots, 1); poly(dA-dG)·poly(dC-dT) (solid curve, 2); poly(dG)·poly(dC) (connected squares, 3). (B) Poly(dA-dT)·poly(dA-dT) (dots, 1); poly(dA-dC)·poly(dG-dT) (solid curve, 2); poly(dG-dC)·poly(dG-dC) (connected squares, 3).

$w > 1$ have been obtained for MTR titrations to the guanine-containing polynucleotides except poly(dA-dC)·poly(dG-dT).

The results of these equilibrium binding studies appear to be supported by the difference CD spectral measurements as shown in Figure 5. The negligible binding of poly(dA-dT)·poly(dA-dT) to MTR is apparent from its spectrum, which is nearly identical with that of MTR in buffer, exhibiting negative and positive CD maximum at 295 and 280 nm, respectively. The binding of MTR to DNA is accompanied by

an intensity enhancement at 445 nm and the generation of a strong exciton-type couplet with positive and negative CD maxima appearing at 285 and 275 nm, respectively, as shown by poly(dG-dC)·poly(dG-dC), poly(dG)·poly(dC), and poly(dA-dG)·poly(dC-dT). The considerably weaker binding of poly(dA-dC)·poly(dG-dT) is also evidenced by its CD features not being greatly different from that of MTR in buffer.

Discussion

Equilibrium binding studies of mithramycin with DNA in the absence and in the presence of a second drug suggest that (1) the drug binds to CT DNA with a binding constant of about 0.3 μM^{-1} (roughly 6–7 times weaker than EB) and saturates at about 1 drug molecule for every 3.3 base pairs; (2) Scatchard plots with unusual curvatures are obtained for the MTR–DNA titrations in the presence of netropsin, a minor-groove binder; (3) the presence of phosphate group binder methylviologen or benzylviologen, on the other hand, induces little effect on the DNA binding characteristics of MTR; and (4) its DNA binding ability is not significantly affected by the presence of major-groove binder spermine or spermidine. The unusual curvature exhibited by the Scatchard plots for the MTR titrations in the presence of netropsin indicates that the binding of netropsin greatly affects the MTR binding to DNA. Since netropsin is a minor-groove binder, its interference with the MTR binding is consistent with the notion that MTR also binds at the minor groove. The interesting curvature can be accounted for by incorporating the binding of the second drug to DNA in the formalism. Binding constants of both drugs can then be extracted from nonlinear least-squares fits of the curved Scatchard plots.

Qualitatively, the unusual curvature in the Scatchard plot may be rationalized in terms of our titration scheme as follows: Since netropsin binds to the DNA minor groove more strongly than MTR and MTR needs about 4 base pairs for binding, most of the A·T-rich sites will be occupied by netropsin at low DNA concentrations, which leaves only a few G·C-rich sites of sufficient length to accommodate the MTR molecules, thus exhibiting lower than normal r values initially. As more DNA is added, more sites not occupied by netropsin become available and, hence, r values increase. However, a point will be reached where sufficient number of free sites are available for MTR binding, and a further increase in the DNA concentration will reduce the r value with a concomitant increase in r/m (normal Scatchard plot). For higher concentrations of netropsin such as 100 μM, this limiting concentration of DNA would be higher and appeared to have not been reached in our titrations.

Our results further indicate that the binding of ethidium to DNA is also significantly affected by netropsin. In contrast to MTR, however, the Scatchard plots in the presence of netropsin do not exhibit unusual curvature but they do exhibit significant decreases in the slopes of the isotherms and nearly identical n values. This difference may be due to the intercalative nature of ethidium binding and the requirement for only 2 base pairs. Since netropsin is strongly A·T specific, whereas ethidium exhibits little base preference, there will be a significant number of gaps, especially the G·C-rich ones, which can accommodate ethidium at most of the DNA concentrations to result in a normal-looking Scatchard plot, except for the reduced slope. Although our results do not shed light on the binding mode of MTR (intercalative vs groove binding), it is interesting to note that fluorescence binding studies of ethidium in the presence of intercalative drugs quinacrine and actinomycin D had earlier been carried out by LePecq et al. (1967). Their results indicate that in the case of weaker binding quinacrine ethidium binds competitively, thus resulting in Scatchard plots of varying slopes but the same n values; in the case of stronger binding actinomycin D, ethidium binds noncompetitively and results in Scatchard plots of identical slopes but varying r intercepts. Our ethidium–netropsin results appear to be more akin to the competitive binding model.

Our finding that both MV and BV exhibit only slight effects on the interaction of MTR or EB with DNA is consistent with the notion that these two positively charged compounds bind at the phosphate groups rather than at the minor groove and thus do not interfere with the presumed groove-binding mode of MTR and the intercalative binding mode of ethidium. Fromhertz and Rieger (1986) had also found that the binding constant of intercalated EB dropped only slightly in the presence of 100 μM MV. They assign the binding of MV to a condensation around the double helix with possible accumulations in the grooves.

Consistent with the guanine specificity of this drug and observations made by others (Baguley, 1982), our polynucleotide results suggest that poly(dG-dC)·poly(dG-dC), its methylated analogue, and poly(dG)·poly(dC) exhibit the greatest affinities for MTR, and their binding strengths do not appear to differ greatly. The saturation binding densities, however, are significantly different with 1 drug molecule per every 1.6 base pairs in the alternating polymer vs 1 drug molecule per every 2.7 base pairs in the homopolymer. On the other hand, much stronger binding is exhibited by poly(dA-dG)·poly(dC-dT) as compared to poly(dA-dC)·poly(dG-dT), and the former binds every 2.5 base pairs, whereas the latter binds every 5–6 base pairs.

The high saturating binding densities observed for DNA in general and for poly(dG-dC)·poly(dG-dC) and poly(dG-m^5dC)·poly(dG-m^5dC) in particular are rather unexpected, as MTR contains extended side chains and will surely cover more than 3 base pairs. These results had troubled us for a long time until the recent appearance of a detailed NMR study on the chromomycin A_3 binding to d(TTGGCCAA)$_2$ (Gao & Patel, 1989). Their results suggest that this antitumor agent binds as a symmetrical dimer to the self-complementary duplex. The two chromomycin molecules in the dimer share the minor groove at the GGCC segment in such a way that each hydrophilic edge of the chromophore is located next to the G-G·C-C half-site and each C-D-E trisaccharide chain extends toward the 3′ direction of the octanucleotide duplex. In addition, the A-B disaccharide segment and the hydrophilic side chain of the antitumor agent are directed toward the phosphate backbone. It was also demonstrated that such a binding requires DNA conformational transformation at its G·C-rich minor groove. The specificity of the chromomycin dimer for G·C-rich regions appears to be associated with a pair of intermolecular hydrogen bonds that can form between the C8 hydroxyl of the chromophore and the N3 (acceptor) and NH_2 (donor) groups on guanosine.

The results of our binding studies in the presence of second drugs are in line with the minor-groove binding of MTR, and our observation of strong exciton-type couplets with respective positive and negative CD maxima appearing at 285 and 275 nm upon binding of MTR to DNA strongly supports the notion of drug dimer in the complex formation. The saturation binding density for poly(dG)·poly(dC) now translates into 1 drug–dimer per 5.4 base pairs in the dimer model, in excellent agreement with the binding site size of 4–5 base pairs found by Gao and Patel (1989) and is consistent with the results from footprinting experiments indicating that the preferred binding sites of MTR and its related antibiotics are at least 3 base pairs long (Van Dyke & Dervan, (1983). It should be pointed out,

however, that the higher saturation binding density of 1 drug–dimer per about 3.3 base pairs for poly(dG-dC)·poly(dG-dC) and poly(dG-m^{5}dC)·poly(dG-m^{5}dC) is more closely packed than the site size of 4–5 base pairs. Although no ready explanation is forthcoming, the possibility of more compact drug–dimer conformations at the CGCG sites and/or dimer overlaps in the alternating polymers cannot be ruled out.

The saturation binding density of 1 drug–dimer per 5 base pairs for poly(dA-dG)·poly(dC-dT), similar to that of poly(dG)·poly(dC), is also somewhat puzzling in view of the G·C specificity of MTR. However, in their chromomycin–d(TTGGCCAA) study, Gao and Patel (1989) pointed out that the presence of the guanosine residue at the central binding site such as G4 is indispensable, but no evidence is found for direct strong interactions between the G3 and the drug molecule in the complex. Thus, the requirement for adjacent G·C base pairs is seen to be somewhat relaxed, which explains the high binding density observed in poly(dA-dG)·poly(dC-dT). The much lower MTR binding affinity and saturation binding density for poly(dA-dC)·poly(dG-dT) as compared to poly(dA-dG)·poly(dC-dT) is likely the consequence of conformational differences of these two sequence isomers.

Finally, parallel DNA binding studies with the related chromomycin A_3 have also been investigated by us. The results are very similar to those found for mithramycin.

Registry No. MTR, 97666-60-9; MV, 1910-42-5; BV, 1102-19-8; EB, 1239-45-8; NT, 1438-30-8; SPD, 124-20-9; SPM, 71-44-3; poly(dA-dT)·poly(dA-dT), 26966-61-0; poly(dA)·poly(dT), 24939-09-1; poly(dG)·poly(dC), 25512-84-9; poly(dG-dC)·poly(dG-dC), 95754-57-7; poly(dA-dG)·poly(dC-dT), 53232-17-0; poly(dA-dC)·poly(dG-dT), 55684-99-6; poly(dG-m^{5}dC), 51853-63-5.

References

Baguley, B. C. (1982) *Mol. Cell. Biochem. 43*, 167–181.

Basu, H. S., Shafer, R. H., & Marton, L. J. (1987) *Nucleic Acids Res. 15*, 5873–5886.

Behr, W., & Hartmann, G. (1965) *Biochem. Z. 343*, 519–527.

Behr, W., Honikel, K., & Hartman, G. (1969) *Eur. J. Biochem. 9*, 82–92.

Benesi, H. A., & Hildebrand, J. H. (1949) *J. Am. Chem. Soc. 71*, 2703–2707.

Buys, C. H. C. M., & Osinga, J. (980) *Exp. Cell Res. 125*, 105–109.

Coleman, A. W., & Goff, L. J. (1985) *Stain Technol. 60*, 145–154.

Coleman, A. W., Maguire, M. J., & Coleman, J. R. (1981) *J. Histochem. Cytochem. 29*, 959–968.

Dalgleish, D. G., Fey, G., & Kersten, W. (1974) *Biopolymers 13*, 1757–1766.

Dasgupta, D., Shashipabha, B. K., & Podder, S. K. (1979) *Indian J. Biochem. Biophys. 16*, 18–21.

Drew, H. R., & Dickerson, R. E. (1981) *J. Mol. Biol. 151*, 535–556.

Elias, E. G., & Evans, J. T. (1972) *J. Bone Jt. Surg. 54A*, 1730–1736.

Fok, J., & Waring, M. J. (1972) *Mol. Pharmacol. 8*, 65–74.

Fox, K. R., & Howarth, N. R. (1985) *Nucleic Acids Res. 13*, 8695–8714.

Fromher, P., & Reiger, B. (1986) *J. Am. Chem. Soc. 108*, 5361–5362.

Gao, X., & Patel, D. J. (1989) *Biochemistry 28*, 751–762.

Gause, G. F. (1965) *Adv. Chemother. 2*, 179–195.

Goldberg, I. H., & Friedman, P. A. (1971) *Annu. Rev. Biochem. 40*, 775–810.

Groyer, A., & Robel, P. (1980) *Anal. Biochem. 106*, 262–268.

Hamilton, V. T., Habbersett, M. C., & Herman, C. J. (1980) *J. Histochem. Cytochem. 28*, 1125–1128.

Hauser-Urfer, I., Leeman, U., & Ruch, F. (1982) *Exp. Cell. Res. 142*, 445–459.

Hill, G. J., Sendransk, N., & Rochlin, D. (1972) *Cancer 30*, 900–908.

Illrionova, R. P., Dykhovichnaya, D. E., & Bondarenko, B. N. (1970) *Antibiotiki (Moscow) 15*, 415.

Keniry, M. A., Brown, S. C., Berman, E., & Shafer, R. H. (1987) *Biochemistry 26*, 1058–1067.

Kennedy, B. J. (1970) *Cancer 26*, 755–766.

Kennedy, B. J., Yarbo, J. W., Kickertz, V., & Sandberg-Wollheim, M. (1968) *Cancer Res. 28*, 91–97.

Kersten, W., Kersten, H., & Szybalski, W. (1966) *Biochemistry 5*, 236–244.

Kersten, W., Kersten, H., Steiner, F. E., & Emmerich, B. (1967) *Z. Physiol. Chem. 348*, 1415–1423.

Klotz, I. M., & Hunston, D. L. (1971) *Biochemistry 10*, 3065–3069.

LePecq, J. B., & Paoletti, C. (1967) *J. Mol. Biol. 27*, 87–106.

Marquet, R., & Houssier, C. (1988) *J. Biomol. Struct. Dyn. 6*, 235–246.

McGhee, J. D., & von Hippel, P. H. (1974) *J. Mol. Biol. 86*, 469–589.

Muller, W., & Crothers, D. M. (1968) *J. Mol. Biol. 35*, 251–290.

Muller, W., & Crothers, D. M. (1975) *Eur. J. Biochem. 54*, 267–277.

Nayak, R., Sirsi, M., & Podder, S. K. (1973) *FEBS Lett. 30*, 157–162.

Nayak, R., Sirsi, M., & Podder, S. K. (1975) *Biochim. Biophys. Acta 378*, 195–204.

Prasad, K. S., & Nayak, R. (1976) *FEBS Lett. 71*, 171–174.

Ream, N. W., Perlia, C. P., Wolter, J., & Taylor, S. G. (1968) *JAMA, J. Am. Med. Assoc. 204*, 96–102.

Schmechel, D. E. V., & Crothers, D. M. (1971) *Biopolymers 10*, 465–480.

Van Dyke, M. W., & Dervan, P. B. (1983) *Biochemistry 22*, 2373–2377.

Ward, D. C., Reich, E., & Goldberg, I. H. (1965) *Science 149*, 1259–1263.

Ware, B. R., Klein, J. W., & Zero, K. (1988) *Langmuir 4*, 458–463.

Waring, M. (1970) *J. Mol. Biol. 54*, 247–279.